JCTC Journal of Chemical Theory and Computation

Article

pubs.acs.org/JCTC

Solvent Effects on the Absorption Spectra of the *para*-Coumaric Acid Chromophore in Its Different Protonation Forms

Francisco F. García-Prieto,[†] Ignacio Fdez. Galván,[†,‡] Aurora Muñoz-Losa,[†] Manuel A. Aguilar,*[,†] and M. Elena Martín*[,†]

[†]Química Física. Edif. José María Viguera Lobo, Universidad de Extremadura, Avda. de Elvas s/n, 06071 Badajoz, Spain

[‡]Department of Chemistry, Ångström, The Theoretical Chemistry Programme, Uppsala University, P.O. Box 518, SE-751 20 Uppsala, Sweden

Supporting Information

ABSTRACT: The effects of the solvent and protonation state on the electronic absorption spectrum of the *para*-coumaric acid (pCA), a model of the photoactive yellow protein (PYP), have been studied using the ASEP/MD (averaged solvent electrostatic potential from molecular dynamics) method. Even though, in the protein, the chromophore is assumed to be in its phenolate monoanionic form, when it is found in water solution pH control can favor neutral, monoanionic, and dianionic species. As the pCA has two hydrogens susceptible of deprotonation, both carboxylate and phenolate monoanions are possible. Their relative stabilities are strongly dependent on the medium. In gas phase, the most stable isomer is the phenolate while in aqueous solution it is the carboxylate, although the population of the phenolate form is not negligible. The s-*cis*, s-*trans*, *syn*, and *anti* conformers have also been included in the study. Electronic excited states of the chromophore have been characterized by SA-CAS(14,12)-PT2/cc-pVDZ level of theory. The bright state corresponds, in all the cases, to a $\pi \rightarrow \pi^*$ transition involving a charge displacement in the system. The magnitude and direction of this displacement depends on the protonation state and on the environment (gas phase or solution). In the same way, the calculated solvatochromic shift of the absorption maximum depends on the studied form, being a red shift for the neutral, carboxylate monoanion, and dianionic chromophores and a blue shift for the phenolate monoanion. Finally, the contribution that the solvent electronic polarizability has on the solvent shift was analyzed. It represents a very important part of the total solvent shift in the neutral form, but its contribution is completly negligible in the mono- and dianionic forms.

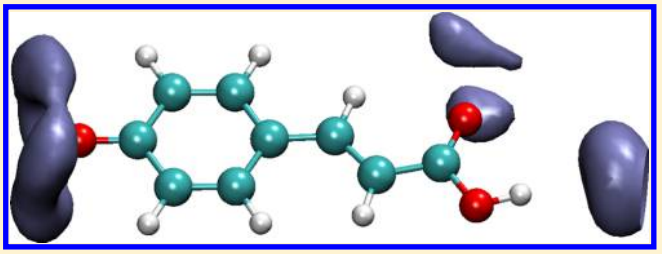

1. INTRODUCTION

Because of its importance for living beings, it is of great interest to understand how the interaction with light can trigger so many different processes in biological systems. Probably, two of the most relevant and amazing processes that can be cited are the vision process and the movement of microorganisms toward or away from an irradiation source, as found in several eubacteria. In this case, light triggers a motor response of the organism called phototaxis, negative if the bacterium moves toward less illuminated areas or positive if the shift is toward the light. The photoreceptor protein related with the negative phototaxis of *Halorhodospira halophila*,[1] under blue light irradiation, is the photoactive yellow protein (PYP).[2,3] This is a small and water-soluble protein, formed by 125 amino acids and a prosthetic group or chromophore, the *trans-p*-coumaric acid, covalently linked to the protein via a thioester bond to Cys69. According to resonance Raman spectra,[4] in the ground state, the chromophore is in the phenolate *trans* form, the negative charge being stabilized by hydrogen bond interactions with the network formed by the surrounding amino acids Tyr42, Glu46, and Thr50. After irradiation (446 nm), the photoprotein enters a photocycle where the primary event is the isomerization of the chromophore's double bond[5−8] on a subpicosecond time scale, very similar to retinal photoisomerization in the visual process.[9] The comprehension of the key interactions leading to the isomerization mechanism needs the complementary effort of experimental and theoretical studies of the chromophore in different environments: gas phase, solution, and inside the protein.

A first, evidence of the medium effect on the pCA chromophore is found in the absorption spectrum. In gas phase, the *p*-coumaric monoanion (pCA^-) absorbs at 430 nm[10,11] whereas in water solution the absorption maximum varies with the pH[11,12] being located at around 310, 283, and 334 nm at acid (pCA), neutral (pCA^-), and basic (pCA^{2-}) conditions. It is important to note that pCA has two hydrogens susceptible of deprotonation and in solution the carboxylic hydrogen is more acid than the phenolic one. Thus, in passing from acidic to neutral condition, the chromophore will first lose the carboxylic hydrogen yielding the carboxylate anion rather than the phenolate. Nevertheless, in gas phase, the phenolate anion is found to be more stable than the carboxylate due to the possibility of delocalizing the negative charge along the

Received: February 26, 2013
Published: August 14, 2013

   dx.doi.org/10.1021/ct400145z | J. Chem. Theory Comput. 2013, 9, 4481−4494

structure, whereas in the carboxylate the negative charge remains on the carboxylic fragment, according to the resonance structures proposed for pCA^- in Figure 1. So, the comparison

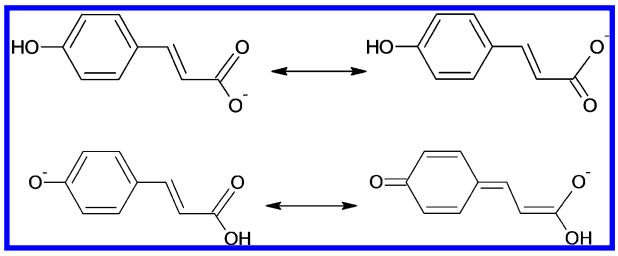

Figure 1. Resonance forms of the monoanion pCA^-. Carboxylate at the top and phenolate at the bottom.

of the absorption maxima in different environments must be performed carefully. In order to ensure that the phenolate anion is the monoanionic form present, other pCA derivatives have been studied. In this way, the deprotonated *trans*-thiophenyl-*p*-coumarate (pCT^-) in gas phase absorbs at 460 nm[11] whereas in water solution the maximum is blue-shifted until 395 nm.[11] Comparing these results with the protein absorption, it can be observed that by passing from gas phase (460 nm) to the protein (446 nm) and finally to water solution (395 nm), the absorption is gradually blue-shifted.

In this work, we have focused in the study of the changes induced by the solvent on the absorption spectra of a model of the PYP chromophore. Even though several models have been employed both in theoretical and experimental studies, most of the efforts have been oriented to the anionic esters and thioesters ($O-CH_3$, $S-CH_3$, S−Ph), ketone (CH_3), and amide (NH_2) derivatives. Comparatively, less attention has been paid to the carboxylic derivative (COOH) probably due to the difficulty of having two possible monoanionic forms, the phenolate and the carboxylate, depending on the conditions of the experimental study. By using action spectroscopy coupled with ion-storage ring and electrospray techniques, the gas-phase absorption spectra of pCA^-, pCT^- (the anionic thiophenyl ester derivative), and $OMpCA^-$ (the anionic methyl ester derivative) have been registered.[10,11,13] For Rocha-Rinza et al.,[10] the in vacuum absorption spectra of phenolate and carboxylate anions are coincident, both maxima being located at around 430 nm. Nevertheless, most of the available theoretical methods[10,14,15] lead to very different values for these maxima. The aug-MCQDPT2 is the only one that provides excitation energies for both anions that are within 0.1 eV of the experimental peaks.[10] It is important to note that the calculated maximum for the phenolate anion agrees with the experimental value while that corresponding to the carboxylate deviates to larger excitation energies. This discrepancy is most likely due to some problems with the experiment or its interpretation. For instance, Zuev et al.[15] suggest contamination of the carboxylate sample by the phenolate isomer. The latter presents much larger oscillator strength and traces of it in the carboxylate sample could result in relatively large absorption. In any case, this disagreement between calculations and experiments remains nowadays an unresolved challenge.

Another point to take into account is the metastable character of the anionic excited states of pCA in gas phase. This means that the lowest excited states of the monoanions are above the detachment continuum and consequently they are autoionizing resonance states.[15−17] A correct treatment of these metastable states needs a good representation of their interaction with the continuum, as it is done, for instance, by methods including complex absorption potential[18,19] and complex-scaling methods.[20−23] This is one of the reasons why the comparison between the vertical excitation energies obtained by experimental and theoretical techniques in gas phase must be treated carefully. In any case, the ionization potential is displaced to higher energies when the calculation is performed in the presence of two water molecules[16] close to the phenolic oxygen (with the intent of mimicking solvent interactions) or an arginine[17] at the position occupied by the Arg52 in the protein environment (in the protein, this amino acid has been thought to be responsible for the stabilization of the negative charge of the chromophore).

Even if there exist a great number of theoretical calculations in gas phase, this is not the case for theoretical studies in solution. In fact, apart from the experimental studies, not many theoretical results in solution can be found in the literature, and in general, they use microhydratation[24] or continuum methods to describe the solvent.[25−28] It is our aim in this work to perform a detailed study of the differences between the absorption spectra in gas phase and in solution of the different protonation states of the pCA, Figure 2. Given the experimental

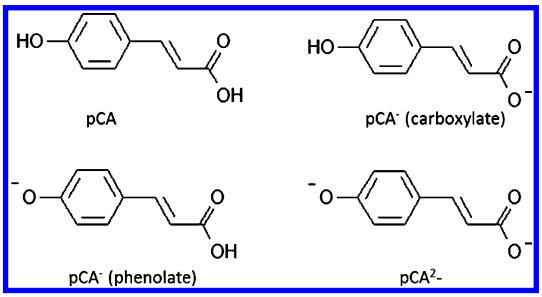

Figure 2. Possible neutral, monoanionic, and dianionic forms of the *p*-coumaric acid.

study[12] of the absorption spectra of pCA in different pH conditions, we regard this study as an opportunity of comparing theory and experiment of the same system. The in water solution calculations will be performed by making use of the ASEP/MD[29] method, a QM/MM method that permits to combine a microscopic description of the solvent with a high-level quantum mechanics treatment of the solute, following the philosophy of sequential QM/MM methods (see the Method section and references therein). In addition, the comprehension of the interaction between the chromophore and the solvent is a valuable piece for solving the puzzling role of the protein's active site on the mission designed by nature for the PYP.

2. METHOD AND COMPUTATIONAL DETAILS

2.1. Method. Over the last two decades, our research group has developed a computational method oriented to the study of solvent effects. This method is known as ASEP/MD,[29−32] acronym for averaged solvent electrostatic potential from molecular dynamics. As a starting and reference point, the main requirements the method had to fulfill were to provide an accurate, quantum-mechanical, treatment of the solute, a microscopic description of the solvent, which accounts for the possible specific interactions between solute and solvent, and, additionally, an affordable computational cost. To achieve this, the ASEP/MD method makes use of the mean field approximation[33,34] (MFA). In this approximation, instead of

considering specific solvent configurations, the perturbation enters into the solute molecular Hamiltonian in an averaged way. Consequently, ASEP/MD through the MFA permits to reduce the number of quantum calculation from several thousands, as usual in QM/MM[35] methods, to only a few, and the highest levels of theory available at present can be employed. Obviously, the prize to pay is missing the information about the absorption band broadening, a common shortcoming for all methods under the MFA. Nevertheless, it is possible to recover part of this information, although we have not done that in this work.[36] The way in which ASEP/MD engages quantum calculations and molecular dynamics simulations in the context of the MFA is sequential,[37] that is, from a fully MM molecular dynamics simulation[38] an averaged solvent representation is obtained, and it is introduced as point charges into the quantum calculation of the solute. Once the associated Schrödinger equation has been solved, the updated solute charge distribution is used in a new molecular dynamics simulation. MM simulations and quantum calculations are successively iterated until the charge distribution of the solute and the solvent structure around it become mutually equilibrated. Other sequential QM/MM methods using the MFA are RISM/SCF,[39−41] ASEC/MC,[42] MF-QM/MM,[43] and methods based in the frozen density embedding theory (FDET).[44] The main difference between them is the way in which the averaged representation of the solvent is obtained and introduced in the QM calculations.

As usual in QM/MM[35] methods, the ASEP/MD Hamiltonian is partitioned into three terms

$$\hat{H} = \hat{H}_{QM} + \hat{H}_{MM} + \hat{H}_{int} \tag{1}$$

corresponding to the quantum part, $\hat{H}_{QM}$, the classical part, $\hat{H}_{MM}$, and the interaction between them, $\hat{H}_{int}$

The energy and the wave function of the solvated solute molecule are obtained by solving the effective Schrödinger equation:

$$(\hat{H}_{QM} + \langle \hat{H}_{int} \rangle)|\Psi\rangle = \bar{E}|\Psi\rangle \tag{2}$$

where the brackets denote a statistical average.

From a computational point of view, it is convenient to split the interaction term into two components associated to the electrostatic and van der Waals contributions:

$$\langle \hat{H}_{int} \rangle = \langle \hat{H}_{int}^{elect} \rangle + \langle \hat{H}_{int}^{vdw} \rangle \tag{3}$$

In general, it is assumed that the van der Waals contribution has little effect on the solute wave function, and therefore, it is usual to represent it through a classical potential that depends only on the solute−solvent nuclear coordinates. It may then be omitted from the electronic Schrödinger equation, but it will obviously contribute to the final value of the energy, and energy derivatives. In our case, a Lennard-Jones potential was used.

Therefore, in our model, only the electrostatic MFA term enters into the electron Hamiltonian, and it is defined as[30,33,34]

$$\langle \hat{H}_{int}^{elect} \rangle = \int d\mathbf{r} \cdot \hat{\rho} \langle V_S(r;\rho) \rangle \tag{4}$$

where $\hat{\rho}$ is the solute charge density operator and $\langle V_S(r;\rho) \rangle$ is the averaged solvent electrostatic potential (ASEP) generated by the solvent at the position r. As indicated, the ASEP depends on the solute charge distribution, and as it changes for successive molecular simulations, the ASEP/MD process must be iterated until convergence is achieved.

In addition to the description of the mutual polarization of the solute and the solvent through its iterative process, ASEP/MD is able to locate critical points on free-energy surfaces and calculate free-energy differences between different solute structures. For geometry optimization in solution, a technique based on the use of the free-energy gradient method[45−48] is employed.

Once the stationary points are located in solution, their relative stability must be determined. With the ASEP/MD methodology, the free-energy difference in solution between two given states is written as the sum of two terms,[49]

$$\Delta G = \Delta E_{solute} + \Delta G_{int} \tag{5}$$

ΔE_{solute} is the internal energy difference between the two solute states at QM level defined as

$$\Delta E_{solute} = E_B - E_A = \langle \Psi_B | \hat{H}_{QM}^{B} | \Psi_B \rangle - \langle \Psi_A | \hat{H}_{QM}^{A} | \Psi_A \rangle \tag{6}$$

where $\hat{H}_{QM}^{X}$ is the gas-phase Hamiltonian for the state X, and Ψ_X is the electronic wave function of the state X in solution. These wave functions are obtained by solving the effective Schrödinger equation (eq 2), with the solvent influence.

The second term of eq 5, ΔG_{int}, is the difference in the solute−solvent interaction free energy, and it is calculated with the free energy perturbation (FEP) method.[50] It must be noted that, although geometries and charges for the initial and final states of the solute are calculated quantum mechanically with the ASEP/MD method, the ΔG_{int} term is obtained through classical simulations.

A fundamental quantity in the study of solvent effects on the electron spectra is the solvent shift, δ, on the absorption energy, defined as the difference between the transition energy values calculated in solution, E_{exc}, and in gas phase, E_{exc}^{0}.

$$\delta = E_{exc} - E_{exc}^{0} \tag{7}$$

where the different contributions for the calculation of the energy transitions are obtained from eq 2.

This procedure must be modified if the solvent electron polarizability is included. The solvent polarization involves the coupling of the QM solute in the state under study with the electronic polarization of the solvent. To this end, we assigned a molecular polarizability to every solvent molecule, located at its center of mass, and simultaneously replaced the effective solvent charge distribution used in the MD calculation by the ab initio gas-phase values of the solvent molecule. The dipole moment induced on each solvent molecule is a function of the dipole moments induced on the rest of the molecules and of the solute charge distribution, and hence, the electrostatic equation has to be solved self-consistently. The process finishes when convergence in the solute and solvent charge distribution is reached.

The total energy of the system (quantum solute and polarizable solvent) is obtained as[51,52]

$$E = E_{qq} + \frac{1}{2}E_{pq} + E_{\rho q} + \frac{1}{2}E_{\rho p} + E_{dist}^{solute} \tag{8}$$

Here, q refers to the permanent charges of the solvent molecules, p to the induced dipoles on the solvent, and ρ is the solute charge density. The last term in eq 8 is the distortion energy of the solute, that is, the energy spent in polarizing it.

The different contributions are[53]

$$E_{qq} = \frac{1}{2}\sum_i q_i V_i^q$$

$$E_{pq} = \sum_i \vec{p}_i \cdot \vec{D}_i^q$$

$$E_{\rho q} = \sum q_i V_i^\rho$$

$$E_{\rho p} = \sum p_i \vec{D}_i^\rho$$

$$E_{\text{dist}}^{\text{solute}} = \langle \Psi | \hat{H}_{\text{QM}} | \Psi \rangle - \langle \Psi^0 | \hat{H}_{\text{QM}} | \Psi^0 \rangle \quad (9)$$

where Ψ and Ψ^0 are in solution and in vacuo solute wave functions, respectively, and V_i^p and V_i^q are the electrostatic potentials generated by the solute charge distribution and by the permanent charges of the solvent, respectively. The electric field generated by the solute and solvent permanent charges are, respectively, $\vec{D}_i^\rho$ and $\vec{D}_i^q$.

Once the solvation energy has been calculated for the ground and excited states, the solvent shift, δ, reads now

$$\delta = \frac{1}{2}\delta_{pq} + \delta_{\rho q} + \frac{1}{2}\delta_{\rho p} + \delta_{\text{dist}}^{\text{solute}} \quad (10)$$

The term δ_{qq} cancels out because, in vertical transitions where the Franck−Condon approximation is applicable, the E_{qq} term takes the same value in both the ground and the excited state; that is, the equilibrium solvent structure is only calculated for the ground state. From a practical point of view, that means that the first self-consistent process is carried out just for the ground state. However, the second cyclic process that permits the response of the electron degrees of freedom of the solvent is carried out for both the ground and the excited states. Further details can be found elsewhere.[53−55]

2.2. Computational Details. Geometry optimizations of the solute, both in gas phase and in solution, were done with the B3LYP functional[56] in the context of the density functional theory[57] (DFT), using the cc-pVDZ basis set. In solution calculations were performed with the ASEP/MD software[29] using Gaussian09[58] and Moldy[59] programs for quantum calculations and molecular dynamics, respectively. Vertical excitation energies were computed with Molcas-7.4[60] with the same basis set. The effect of the electronic solvent polarization on the vertical excitation energy and solvent shift values has been analyzed. For these calculations, the complete active space self-consistent field (CASSCF) multireference theory[61] was used to account for the near-degeneracies of different electronic configurations. The active space included all the π space which entails 14 electron in 12 orbitals. All calculations were performed using a state average (SA) of the first ten singlet states, with equal weights. This can be considered as an unusually large number of roots, but the choice was made in order to keep the same number of roots in calculations for the neutral, monoanionic, and dianionic forms of pCA. As it is known, for gas-phase CASSCF calculations, the bright state of the carboxylate monoanion is very high in energy. In fact, it is the sixth root when a state average of ten states was considered. Nevertheless, we checked that, for the rest of the studied species, the transition energies were almost unaffected when the number of roots in the wave function was reduced to five. For instance, the change in transition energies for the neutral form was around 0.01 eV.

In order to take into account the rest of the correlation energy,[62] called dynamic correlation, a multireference second-order perturbation theory[63,64] (CASPT2) was employed, using the SA(10)-CASSCF(14,12) wave function as reference. Because of the limited size of the basis set and in order to facilitate comparison with experiment, we use a value of 0.0 for the ionization potential−electron affinity (IPEA) shift in the CASPT2 calculation.[65−68] To minimize the appearance of intruder states, an additional imaginary shift of $0.1i\ E_h$ was used. The oscillator strengths were calculated with the RASSI algorithm implemented in Molcas. Test calculations with larger basis sets (cc-pVTZ, aug-cc-pVDZ) showed that the trends, features, and conclusions reported in this work are not significantly affected by the basis set, although the transition energies decrease by 0.2−0.3 eV (see the Supporting Information).

The molecular dynamics simulations included 900 water molecules and one molecule of solute in a cubic box of 30 Å side in order to reproduce the experimental solvent density. All molecules had fixed intramolecular geometry. For the solute, the Lennard-Jones parameters were taken from the optimized potentials for liquid simulations, all atoms (OPLS-AA[69]) force field, and the atomic charges were obtained from the quantum calculations using the CHELPG[70,71] method. For water molecules, the TIP3P[72] model was employed. Periodic boundary conditions were applied and a spherical cutoff was used to truncate interatomic interactions at 11.6 Å. The electrostatic interaction was calculated with the Ewald method,[38] and the temperature was fixed at 298 K with the Nosé−Hoover thermostat.[73] Each simulation was run in the NVT ensemble for 75 ps, with a time step of 0.5 fs, where the first 25 ps were used for equilibration and the last 50 ps for production. In solution final results were obtained by averaging the last five ASEP/MD cycles, and therefore, they represent a 250 ps average.

The variation of the electron density upon vertical transitions has been calculated with Molden[74] from the CASSCF wave functions. In the three-dimensional maps, the electron flux goes from the blue part toward the red one, that is, blue for a decrease in density and red for an increase.

3. RESULTS

3.1. Neutral Species. For the neutral form of the *trans-p*-coumaric acid (pCA), four conformers can be proposed. Two of them attending to the *cis* or *trans* disposition of the central vinyl double bond and the carboxylic double bond of the acid terminal group, s-*cis* and s-*trans*. For each of these species, the hydrogen of the phenolic group can be disposed in *syn* or *anti* position relative to the central double bond. These four species are displayed in Figure 3 and are identified as I (s-*cis*-*anti*), II (s-*cis*-*syn*), III (s-*trans*-*anti*) and IV (s-*trans*-*syn*).

3.1.1. Solvent-Induced Changes in the Structure, Charge Distribution, and Relative Stability of the Neutral Forms. Gas-phase optimizations lead to planar structures with bond lengths and angles similar for all the neutral species. In all of them, it can be noted a slight quinoidal character of the phenolic ring as the C2−C3 and C5−C6 bonds present a more marked double-bond character than the rest of the ring. For more details about the optimized geometry of the neutral species see the Supporting Information where the geometric parameters of all the studied isomers can be found. With respect to energetic stability of these conformers, see Table 1, the s-*cis* isomer is only 0.8 kcal/mol more stable than the s-*trans* and no differences can be noted between *syn* and *anti* conformers for each of them. Our geometrical and energetic

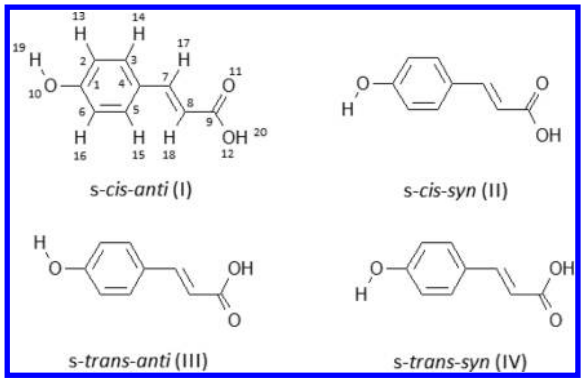

Figure 3. Studied isomers of the neutral *p*-coumaric acid (pCA).

Table 1. Energy Differences for the Different Isomers of the Neutral pCA[a]

	gas phase	water solution		
	ΔE	ΔE_{solute}	ΔG_{int}	ΔG
I (*s-cis-anti*)	0.00	0.00	0.00	0.00
II (*s-cis-syn*)	0.09	0.10	−0.37	−0.27
III (*s-trans-anti*)	0.81	1.14	−0.10	1.04
IV (*s-trans-syn*)	0.84	1.17	−0.69	0.49

[a]Gas-phase and water-solution energies in kcal/mol.

results are analogous to those published by Gromov et al.[75] where the thermodynamically most favorable form for pCA is the *s-cis-syn* isomer and where the difference between *anti* and *syn* isomers is around 0.1 kcal/mol. Regarding the electronic distribution, the total dipole moment of a molecule can be considered as the vector sum of the constituent bond dipole moments. This concept roughly helps in the interpretation of the differences found in the dipole moment of the I to IV ground state forms showed in Table 2. In this way, when the direction of the dipole moment corresponding to the phenolic OH bond is opposite to that showed by the carboxylic C═O bond (*anti* rotamer for the *s-cis* isomer, I, and *syn* rotamer for the *s-trans*, IV), the total dipole moment is lower than when the direction of the two bond dipoles is parallel (*syn* rotamer for the *s-cis* isomer, II, and *anti* rotamer for the *s-trans*, III). By pairs the magnitude of these total dipole moments is similar (I and IV around 1.5 D, and II and III around 2.5−3.0 D).

In water solution, the electronic distribution of the chromophore polarizes as a result of the interaction with the solvent. This polarization evidences itself in the increase of the dipole moment with respect to the gas-phase value. For the I form (see Table 2), the observed increase is 53−77% for S_0 and S_1 states and 40−57% for the S_2 excited state. As for the relative stability of the different isomers, it can be observed that in solution the *s-cis* conformer is still preferred to the *s-trans*, but an inversion of the *syn* and *anti* stability is found. Thus, if in gas phase *anti* rotamers are preferred to the *syn* ones, in solution the opposite is verified and the *syn* conformations are slightly more stable than the *anti*. See ΔG in Table 1. In any case, given the approximations introduced in the calculation and the low value of the free-energy differences these results must be taken with caution.

Variations in the geometric parameters of the chromophore ground state introduced by the solvent are not very significant and they are similar for all the neutral conformers. As a general trend, double bonds become shorter and single bonds longer. The terminal parts of the chromophore present a larger interaction with the water molecules as they can form hydrogen bonds with it. As a consequence, O−H and C═O bond lengths show larger values in solution than in gas phase. From the analysis of the most representative radial distribution functions, see Figure S1 in the Supporting Information, one can conclude that there are no differences in the equivalent functions of the four isomers.

3.1.2. Solvent Shifts on the Electronic Spectra of the Neutral Forms. As shown in Table 2, the most probable ($\pi \rightarrow \pi^*$) transition in gas phase is the absorption to the S_2 state with an oscillator strength of around 0.5. This is a HOMO → LUMO transition involving a gap of 4.5 and 4.6 eV for the *s-cis* and *s-trans* isomers, respectively. The transition to the S_1 state corresponds to a HOMO → LUMO + 1 transition with an energy gap of around 4.23 eV for all the forms. In Figure 4, the involved orbitals and the three-dimensional maps of the electron density variation upon vertical transitions for $S_0 \rightarrow S_1$ and $S_0 \rightarrow S_2$ of I are displayed. Similar results are obtained for the rest of the neutral forms. The showed orbitals present the same topology as those reported by Gromov et al.[75] The S_0

Table 2. Dipole Moment, Vertical Transition Energy, Oscillator Strength, and Solvent Shift for the Different Neutral Isomers of pCA in Gas Phase and in Solution

	gas phase				water solution				
	I	II	III	IV	I	II	III	IV	exp
				Dipole Moment (D)					
S_0	1.5	2.6	3.1	1.5	2.3	4.3	5.5	2.7	
S_1	1.5	2.6	3.2	1.5	2.4	4.4	5.6	2.8	
S_2	6.8	6.5	7.5	6.4	9.5	10.2	11.5	9.9	
				Vertical Transition (eV)					
$(S_0 \rightarrow S_1)$	4.23	4.23	4.24	4.24	4.22	4.22	4.23	4.22	
$(S_0 \rightarrow S_2)$	4.49	4.52	4.62	4.65	4.33	4.29	4.37	4.36	4.00[a]
				Oscillator Strength					
$(S_0 \rightarrow S_1)$	0.005	0.005	0.005	0.004	0.005	0.005	0.005	0.005	
$(S_0 \rightarrow S_2)$	0.566	0.549	0.583	0.564	0.425	0.425	0.408	0.394	
				Solvent Shift (kcal/mol)					
$(S_0 \rightarrow S_1)$					−0.24	−0.20	−0.31	−0.29	
$(S_0 \rightarrow S_2)$					−3.72	−5.39	−5.77	−6.72	

[a]Ref 12.

dx.doi.org/10.1021/ct400145z | J. Chem. Theory Comput. 2013, 9, 4481−4494

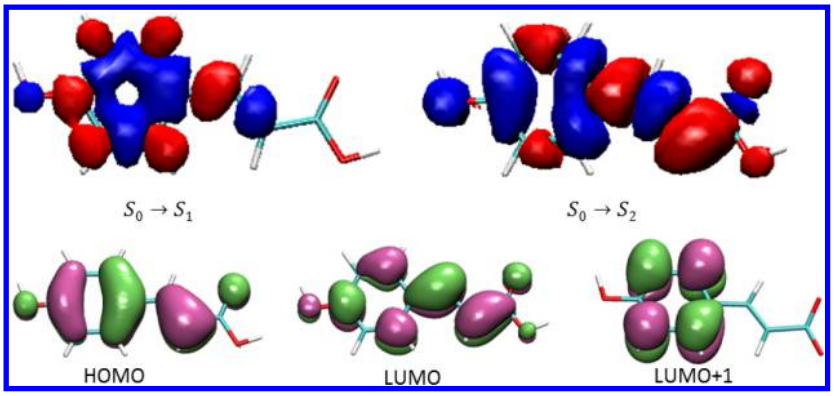

Figure 4. Three-dimensional electron density change maps of the $S_0 \rightarrow S_1$ and $S_0 \rightarrow S_2$ electronic transitions of the neutral pCA. The electronic flux goes from the blue part to the red one. The involved orbitals are depicted as well in green and mauve colors.

$\rightarrow S_2$ transition corresponds mainly to a redistribution of the electronic density at the phenolic ring and from the vinyl double bond toward its two adjacent single bonds. On the contrary, the $S_0 \rightarrow S_1$ transition involves almost exclusively the phenolic ring. If the molecule is divided into three parts (phenolic ring, central double bond and carboxylic group) and the variation of the Mulliken populations during the electron transition is analyzed (see Table S3 in the Supporting Information) it results that the ground and the first excited state show practically the same charge along the three parts whereas in the second excited state there exists a displacement of the negative charge from the phenolic ring to the alkyl fragment. This behavior agrees with an increase of the dipole moment of the S_2 state with respect to the ground and first excited states. It is worth reminding that we only consider Mulliken populations as a means of analyzing electron density changes, but in all simulations CHELPG charges were used, which provide a better representation of the electrostatic interaction between solute and solvent.

Our transition energies are somewhat lower than those published by Gromov et al.[75] (4.84 and 5.13 eV for S_1 and S_2) and Martínez et al.[76] (4.93 and 5.17 eV for S_1 and S_2). The differences are probably due to the different computational conditions followed in each case. Martínez et al. reported CASPT2 (with a CASSCF reference wave function calculated as the state average of 3 or 5 roots, with a reduced active space including 6 electrons in 5 orbitals, and using 0.25 as value for the IPEA shift) and EOM-CCSD results, both of them using the 6-31G* basis set. Similar EOM-CCSD calculations were performed by Gromov et al.[75] In previous papers, we have shown that with larger basis sets, the use an IPEA shift 0.0 tends to result in lower absorption energies while the default value of 0.25 for the IPEA shift usually yields values more similar to other methods.[65−68] This explains the difference between our SA(10)-CAS(14,12)-PT2 (IPEA 0.0) calculations and those of other authors. We nevertheless note that the different calculations agree in the nature of the S_0, S_1, and S_2 states as well as in the energy gap between the two excited states, which ranges between 0.24 and 0.30 eV. However, this difference is notably larger (1.4 eV) in the study of Sergi et al.[77] at TD-DFT with triple-ζ basis set with one polarization function. Consequently, some doubts can arise regarding the suitability of TD-DFT level of calculations for this system.

The shift induced by water in the position of the absorption bands with respect to the gas-phase spectrum (δ) is also showed in Table 2. The experimental transition energy for pCA in acidic water solution has been found at 4.00 eV (310 nm).[12] According to our calculations, the most probable transition is still that corresponding to the S_2 state, with an oscillator strength of 0.4. This transition results in around 4.30 eV, which overestimates the transition in about 0.3 eV if solvent polarization is not considered. On the contrary, if this contribution is included we get a value of 4.00 eV, in perfect agreement with the experiment. The importance of considering the solvent polarizability in electron transitions has been illustrated by several authors.[78−80]

It can be also observed that the $S_0 \rightarrow S_1$ transition is hardly affected by the solvent interaction, being the vertical transition energies in gas phase and in solution practically coincident. This is still the case when solvent polarization is taken into account. The different behavior of S_2 and S_1 in their interaction with the solvent comes from the distinct charge distribution of these states. Whereas the transition to S_2 implies an electron density displacement from the phenolic ring to the alkyl fragment and a considerable increase in the dipole moment, S_1 shares with S_0 similar charge distribution and consequently similar stabilization by the solvent.

Due to the larger stabilization of S_2 with respect to S_1 in water solution, both states become almost degenerate when solvent polarization is not considered. This is not the case when the solvent is allowed to polarize. In this case, S_2 is stabilized by the solvent to an even greater extent and not only the excited states are not degenerate but the bright one becomes the first excited state (transition energy of 4.00 eV vs 4.22 eV).

The solvent shift for the S_1 excited state is strongly reliant on the electronic solvent polarization. So, the red solvent shift value increases from 3.72 to 11.25 kcal/mol for structure I when the electronic solvent polarization contribution is taken into account. A similar behavior is found for the rest of the neutral forms.

3.2. Monoanionic Species. In this section, phenolate and carboxylate monoanions (pCA^-) are analyzed. The forms displayed in Figure 5 have been treated: *anti*-OH, V, and *syn*-OH, VI, rotamers for the carboxylate anion, and s-*cis*, VII, and s-*trans*, VIII, isomers for the phenolate anion. The main resonance structures of the pCA^- are depicted in Figure 1. Whereas in the carboxylate the negative charge is localized on the carboxylate end, in the phenolate anion, the negative charge is spread along the whole molecule. In fact, in phenolate, there is an equilibrium between a quinolic structure with the negative charge localized at the COOH fragment, and a nonquinolic

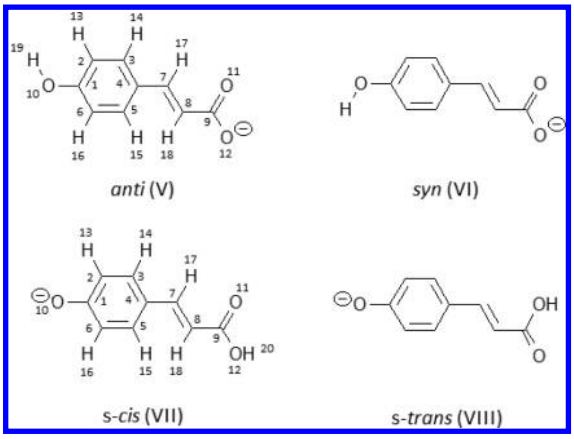

Figure 5. Studied isomers of the monoanionic *p*-coumaric acid (pCA^-).

structure with the negative charge at the phenolate oxygen. We will come back to this aspect later.

3.2.1. Solvent-Induced Differences in the Structure, Charge Distribution, and Relative Stability of Phenolate and Carboxylate Forms. In gas phase, and in agreement with the results found by Rocha-Rinza et al.,[10] the ground state of the phenolate form is clearly more stable than the carboxylate species, see Table 3. In fact, the contribution of the carboxylate form to the conformational equilibrium is completely negligible. *Anti* and *syn* carboxylate rotamers on the one hand and s-*cis* and s-*trans* phenolate isomers on the other hand present very similar stabilities although the *syn* carboxylate and the s-*cis* phenolate are slightly more stable. This behavior is maintained in solution, and for convenience, further tables and figures in this section as well as the results discussion will only refer to the most stable forms of each anion. The results for all the studied isomers can be found in the Supporting Information.

Table 3. Energy Differences for the Different Isomers of the Monoanionic pCA^-[a]

	gas phase	water solution		
	ΔE	ΔE_{solute}	ΔG_{int}	ΔG
V (carboxylate *anti*)	0.00	0.00	0.00	0.00
VI (carboxylate *syn*)	−0.05	0.80	−1.55	−0.75
VII (phenolate s-*cis*)	−19.00	−24.54	26.03	1.50
VIII (phenolate s-*trans*)	−18.45	−23.65	26.01	2.36

[a]Gas-phase and water-solution energies in kcal/mol.

Regarding the geometry, the bond lengths obtained are compatible with the existence of an equilibrium between the resonance forms displayed in Figure 1. In particular, the ground-state carboxylate shows equivalent C9−O11 and C9−O12 bond lengths with intermediate values between typical single and double bond (see the Supporting Information).

In the phenolate anion, the gas-phase optimized geometry for the ground state is a structure with bond lengths intermediate between the two proposed resonance forms. The phenolic ring presents a quinolic structure with C1−O10, C2−C3, and C5−C6 bonds clearly shorter than those corresponding to the carboxylate anion. In turn, in the alkyl fragment, the central double bond (C7−C8) increases its length, unlike the adjacent single bonds whose length decreases, with respect to the values of typical double and single bonds distances, respectively. The study of the charge distribution shows that the negative charge is mainly located at the phenolic part and especially at O10, see Table 4 in the text and Table S12 in the Supporting Information. Some density is shared with the carboxylic end and in a lesser extent with the central double bond part. This fact highlights the role of the two possible resonance forms in gas phase, where the negative charge is located at different ends of the molecule.

Interaction with solvent molecules modifies the relative stability of the different isomers, and in water solution, the carboxylate becomes now the most stable form. However, the population of the phenolate form is not negligible, about 4%. The explanation for this fact lies again in the larger localization of the negative charge in the carboxylate, see Table 5. Unlike in gas phase, where charge localization is unfavored, in polar solvents, the carboxylate is more stabilized by the solvent than the phenolate. Considering the more stable forms of phenolate (s-*cis*) and carboxylate (*syn*) anions, the free energy difference in solution results in around 1.77 kcal/mol.

By analyzing the Mulliken charges for the ground state of the phenolate monoanion, it can be noted that the negative charge over the phenolic oxygen (O10) is larger in solution (−0.71 *e*) than in gas phase (−0.45 *e*). This indicates that now the negative charge is less delocalized along the chromophore, and consequently, the quinolic form must be less prevalent than in gas phase. This hypothesis is confirmed when the change caused by the solvent interaction in the geometrical parameters of the phenolate anion is analyzed: the C1−O10, C2−C3, C5−C6, C4−C7, and C8−C9 bonds lengths increase and the conjugated bonds show the opposite effect. In addition, C1−O10, C9−O11, and O12−H20 bonds are elongated as a consequence of the formation of hydrogen bonds between the O10, O11, and H20 atoms and water molecules. Figure 6(a) displays the rdfs between the oxygen atoms of pCA^- and water. The first remark is that, although in phenolate the rdfs around O10 and O11 have peaks at the same positions, the height is larger in O10, in agreement with the larger negative charge sustained by this atom.

Table 4. Mulliken Charges (*e*) for the Phenolate Monoanion, pCA^-, and the $OMpCA^-$ Ester Calculated at the Same Level of Theory[a]

	gas phase				water solution				
	pCA^-		$OMpCA^-$		pCA^-		$OMpCA^-$		
	S_0	S_1	S_0	S_1	S_0	S_1	S_0	S_1	S_2
$^-$O−Ph	−0.713	−0.517	−0.732	−0.531	−0.845	−0.484	−0.972	−0.908	−0.688
vinylic bond	−0.101	−0.204	−0.105	−0.221	−0.001	−0.197	0.050	0.002	−0.158
COOH	−0.187	−0.280	−0.163	−0.248	−0.154	−0.319	−0.078	−0.090	−0.154

[a]Note that S_2 is the bright state for the ester in solution.

dx.doi.org/10.1021/ct400145z | J. Chem. Theory Comput. 2013, 9, 4481−4494

Table 5. Mulliken Charges (e) for the Carboxylate Monoanion

	gas phase					water solution		
	S_0	S_1	S_2	S_3	S_4	S_0	S_1	S_2
HO−Ph	−0.097	−0.523	−0.173	−0.884	−0.184	−0.038	−0.034	0.081
vinylic bond	−0.097	−0.465	−0.030	−0.178	−0.110	−0.028	−0.030	−0.074
COO^-	−0.807	−0.012	−0.797	0.062	−0.706	−0.935	−0.937	−1.006

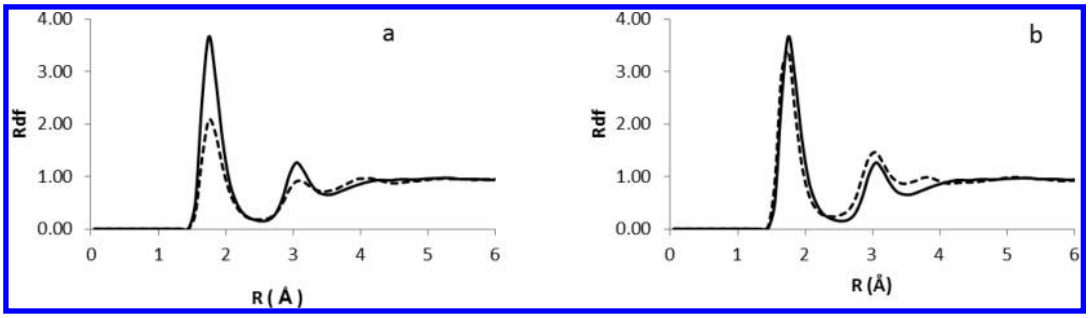

Figure 6. Radial distribution function (rdf) for some atom pairs in phenolate and carboxylate monoanions. O10 phenolate-water hydrogen (full lines) compared with two other rdfs: O11 phenolate-water hydrogen (a, dashed line), O11 carboxylate-water hydrogen (b, dashed line).

In Figure 6(b), it can be observed the similar disposition of the solvent around the O10 in phenolate and O11 in carboxylate, atoms where the negative charge is mainly located in each isomer.

3.2.2. Solvent Shifts on the Electronic Spectra. Before analyzing the solvent effect on the electronic spectra of pCA^-, there are several points that must be clarified. On the one hand, it is important to note that, for both carboxylate and phenolate monoanions, the gas-phase ($\pi \rightarrow \pi^*$) low-lying excited states are found in the detachment continuum, that is, their electron detachment energies are below the first vertical excitation energy,[15] and therefore, these excited states are metastable. This is one of the reasons why the comparison between the vertical excitation energies obtained by experimental and theoretical techniques in gas phase must be treated carefully. Nevertheless, this does not seem to be the case for the chromophore in more complex environments, such as, for instance, in the presence of a counterion or predictably inside the protein cavity. Gromov et al.[17] showed that the ionization potential for the deprotonated *p*-coumaric thio-methyl ester, $pCTM^-$, is shifted to higher energies when two water molecules in the proximity of the phenoxy oxygen are included or in the presence of Arg52 (in the protein, this amino acid has been thought to be responsible for the stabilization of the negative charge of the chromophore). It is our aim, in the present section, to analyze the absorption band shift when the interaction with the solvent is taken into account, and it is in this context that the transition energies calculated in gas phase must be considered.

On the other hand, as it has been already indicated, there are important discrepancies between the absorption spectra of the pCA^- carboxylate monoanion in gas phase obtained through experimental and theoretical studies. This fact was already mentioned in the original experimental/theoretical paper of Rocha-Rinza el al.[10] The experiment places the gas-phase absoption maxima of the carboxylate and phenolate anions at 2.88 eV whereas most of the more accurate ab initio calculations agree in a blue-shifted position of the carboxylate maximum with respect to the corresponding to the phenolate anion. Only the aug-MCQDPT2 method provides absorption maxima similar for both anionic forms.[10] In our opinion, more tests should be run in order to check the realibility of these results. With this, most of the theoretical results point to an error in the experimental data. Zuev at al.[15] suggested contamination of the carboxylate sample by trace amount of the phenolate form, and consequently, they propose a revision of the experiment by probing higher energies for the spectrum of the carboxylate anion.

As it will be seen below, our CASPT2//B3LYP/cc-pVDZ results provide a difference of 2.1 eV between the gas-phase transition energies of carboxylate and phenolate, in agreement with MRMP2/d-aug-cc-pVDZ results.[10] Given the existing uncertainties on the interpretation of the experimental electronic spectra in gas phase and considering the good agreement between the calculated excitation energy for phenolate (2.89 eV) and the experimental data (2.88 eV),[10] we consider the CASPT2//B3LYP/cc-pVDZ level of calculation employed in this paper as valid.

In Table 6 are collected the transition energies in gas phase and in water solution as well as the solvent shift calculated for both *syn* carboxylate, VI, and s-*cis* phenolate, VII, monoanions. Results for s-*trans* phenolate and *anti* carboxylate can be found in the Supporting Information.

Phenolate Monoanion. In gas phase, the most probable transition is that leading to the S_1 state, with an oscillator strength of 1.0. This corresponds to a ($\pi \rightarrow \pi^*$) transition involving the HOMO and LUMO orbitals. These orbitals and the corresponding three-dimensional maps of the electron density variation upon vertical transition for $S_0 \rightarrow S_1$ in gas phase are depicted in Figure 7. There exists a displacement of electron density from the phenolic ring to the rest of the molecule. During the $S_0 \rightarrow S_1$ transition, the negative charge on the phenolic part is reduced in ca. 27% and it is accommodated at the other parts of the molecule. This more balanced charge distribution involves a decrease of more than 60% in the excited-state dipole moment from the ground state. As it will be seen later, this charge displacement is opposite to that found in the carboxylate. The displayed orbitals are of similar topology to those published in previous theoretical studies.[15,17]

In gas phase, our calculations provide a value for the energy gap between the ground state and the first excited state of 2.89 eV, in very good agreement with the gas-phase experimental

dx.doi.org/10.1021/ct400145z | J. Chem. Theory Comput. 2013, 9, 4481−4494

Table 6. Dipole Moment, Vertical Transition Energy, Oscillator Strength, and Solvent Shift for the Different Isomers of pCA^- in Gas Phase and in Solution

	gas phase			water solution		
	carbox. (VI)	phen. (VII)	exp	carbox. (VI)	phen. (VII)	exp
			Dipole Moment (D)			
S_0	17.30	5.51		22.01	12.78	
S_1	2.10	1.98		21.91	4.10	
S_2	16.40					
S_3	4.84					
S_4	14.67					
			Vertical Transition (eV)			
$(S_0 \rightarrow S_1)$	3.86	2.89	*a*	4.25	3.09	*b*
$(S_0 \rightarrow S_2)$	4.03			4.76		
$(S_0 \rightarrow S_3)$	4.69					
$(S_0 \rightarrow S_4)$	5.06					
			Oscillator Strength			
$(S_0 \rightarrow S_1)$	0.016	1.002		0.005	0.882	
$(S_0 \rightarrow S_2)$	0.009			0.536		
$(S_0 \rightarrow S_3)$	0.001					
$(S_0 \rightarrow S_4)$	0.499					
			Solvent Shift (kcal/mol)			
$(S_0 \rightarrow S_1)$				5.15	4.81	
$(S_0 \rightarrow S_2)$				−6.72		

[a]For phenolate in gas phase: 2.88 eV (pCA^- and $OMpCA^-$), ref 10, and 2.70 eV (pCT^-), ref 11 For carboxylate in gas phase: 2.88 eV (pCA^-), ref 10. [b]For phenolate in solution: 3.48 eV ($OMpCA^-$), ref 10. For carboxylate in solution: 4.40 eV ($pCMe^-$), ref 10, 4.35 eV (pCA^-), ref 11, and 4.38 (pCA^-), ref 12.

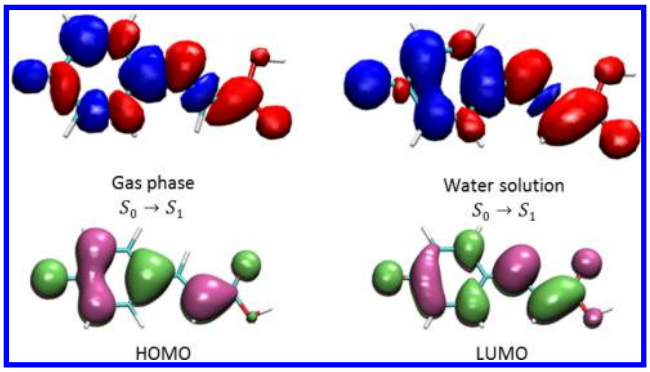

Figure 7. Three-dimensional maps of the $S_0 \rightarrow S_1$ transition in gas phase and in water solution of the phenolate monoanion. The electronic flux goes from the blue part to the red one. The involved orbitals are depicted as well in green and mauve colors.

data (2.88 eV for pCA^- and for the anionic methyl ester derivative,[10] $OMpCA^-$, and 2.70 eV for the anionic thio-phenyl ester derivative,[11] pCT^-) and with other theoretical studies in the literature (2.89 eV for the anionic *p*-coumaric thio-methyl ester,[17] $pCTM^-$, or 2.98 eV for pCA^- with a similar level of calculation[15]).

In water solution, the characteristics of the electronic spectrum are quite similar to those observed in gas phase. The bright state remains the S_1, with the same nature as in gas phase. Nevertheless, the absorption band appears displaced toward larger energies (3.17 or 3.09 eV depending whether the solvent is polarized or not); consequently, there is a blue solvent shift of around 0.25 eV. The only experimental data available refers to the anionic methyl ester derivative of pCA, $OMpCA^-$,[10] in methanol where the absorption maximum is located at around 3.48 eV. Consequently, the experimental blue shift for the ester takes a value of 0.6 eV. To clarify the origin of this discrepancy, we analyze the charge distributions calculated for pCA^- and $OMpCA^-$ and showed in Table 4. Calculations for $OMpCA^-$ have been run at the same level as for pCA^-. In solution, the ground-state negative charge becomes more localized at the phenolic end as this permits a more favorable and stabilizing interaction with the solvent molecules both in pCA^- and $OMpCA^-$. In fact, the ground state suffers an important polarization and its dipole moment increases to 12.78 D (for pCA^-). The excited states are polarized as well by the solvent but in a lower extent; in consequence, they are less stabilized and a final blue shift results. The three-dimensional map of the electron density variation in water solution (Figure 7) is consistent with this explanation.

The *p*-coumaric phenolate monoanion displays a slightly lower blue shift than the methyl ester because during the transition part of the charge is transferred to the carboxylic end and this charge is better solvated in the acid than in the ester. In fact, as it can be observed in Table 4, the negative charge located at the carboxylic end is larger for pCA^- than for $OMpCA^-$.

Carboxylate Monoanion. The theoretical electronic absorption spectrum of the carboxylate anion is quite complex due to the large number of excited states lower in energy than the bright one. In fact, the transition with the larger oscillator strength (0.50) is $S_0 \rightarrow S_4$; see Table 6. This corresponds to a $(\pi \rightarrow \pi^*)$ transition involving the HOMO and LUMO orbitals. Lower in energy are the $H - 1 \rightarrow L$ $(S_0 \rightarrow S_1)$, $H \rightarrow L + 1$ $(S_0 \rightarrow S_2)$ and $H - 1 \rightarrow L + 1(S_0 \rightarrow S_3)$ transitions. Figure 8 displays the involved orbitals and the corresponding three-dimensional maps of the electron density variation upon vertical transition for $S_0 \rightarrow S_1$, $S_0 \rightarrow S_2$, $S_0 \rightarrow S_3$, and $S_0 \rightarrow S_4$. These orbitals show similar topology to those published by Zuev et al.[15] Only the H + 1 orbital presents some differences, although it remains a phenyl ring orbital.

From the electron density variation maps, it seems evident that the $S_0 \rightarrow S_3$ and $S_0 \rightarrow S_1$ transitions are characterized by a charge transfer from the COO^- group to the ring $(H - 1 \rightarrow L + 1)$ or to a more extense zone of the molecule, involving both the ring and the central bond $(H - 1 \rightarrow L)$, respectively. The difference between the dipole moments of the ground state and the S_1 and S_3 states supports the intramolecular charge transfer nature of these states, see Table 6. With an intermediate energy appears the S_2 valence state caracterized by a $H \rightarrow L + 1$ transition. If one compares these orbitals with those of the neutral species, the HOMO, LUMO, and LUMO + 1 present similar characteristics. The most noticeable differences are found in the HOMO − 1 orbital and in the vertical excited states related with it. In any case, from the electron density variation maps it can be observed that the bright transition involves a displacement of electron density from the carboxyl to the hydroxyl. It is important to remark that this displacement is opposite to that reported for the phenolate monoanion.

Significant differences are found when the electronic spectrum is studied in water solution. The most striking fact is that the charge transfer states vanish from among the 10 lowest excited states. Since the carboxylate anion has its negative charge mainly at the COO^- end, the electrostatic interaction with the polar water molecules is quite intense. As a consequence, the charge transfer toward the ring is not favored and these states are shifted to higher energies. In solution, the

dx.doi.org/10.1021/ct400145z | J. Chem. Theory Comput. 2013, 9, 4481−4494

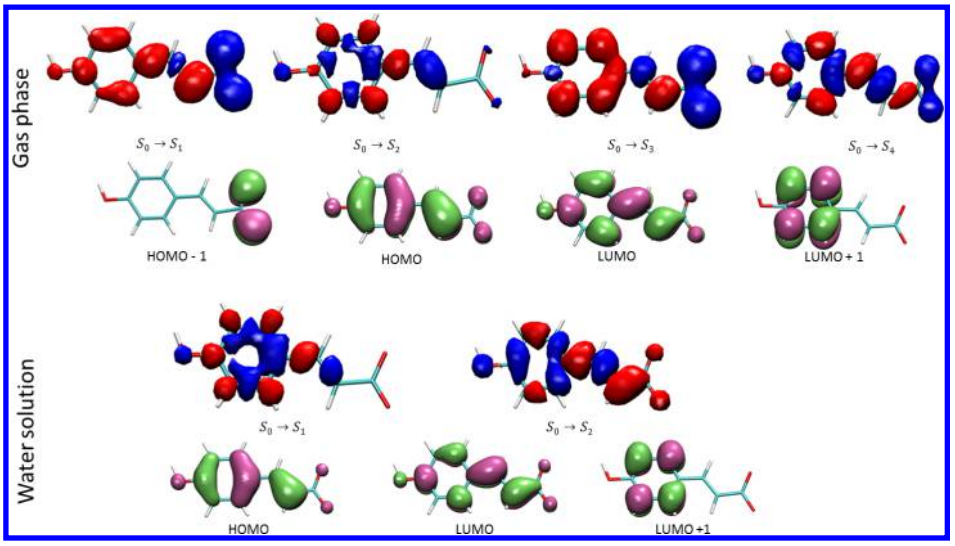

Figure 8. Three-dimensional maps of the studied transitions in gas phase and in water solution of the carboxylate monoanion. The electronic flux goes from the blue part to the red one. The involved orbitals are depicted as well in green and mauve colors.

Table 7. Mulliken Charges (e) for the Dianion, pCA^{2-}

	gas phase			water solution		
	S_0	S_1	S_2	S_0	S_1	S_2
$^{-}$O−Ph	−0.996	−1.040	−0.733	−0.971	−0.619	−0.972
vinylic bond	−0.149	−0.112	−0.371	−0.068	−0.312	−0.067
COO^{-}	−0.856	−0.849	−0.896	−0.962	−1.069	−0.961

first excited state involves a H → L + 1 transition similar to what was found in gas phase for the S_2 state. Nevertheless, in this case, some H − 4 → L contribution can be noted. The bright state is the S_2 excited state. It is a H → L transition, and it has an oscillator strength slightly larger than that found in gas phase. Orbitals involved in the first two electron transitions are displayed in Figure 8.

In gas phase, the transition to the bright state ($S_0 \rightarrow S_4$) involves a displacement of electron density from the carboxylic end to the rest of the molecule. In water solution, where the most intense transition is $S_0 \rightarrow S_2$, the opposite is found. Accordingly, the S_2 excited state is more effectively solvated and more stabilized than the ground state, the transition energy (4.76 eV) is lower than in gas phase (5.06 eV) and a reference solvent shift (0.3 eV) is found.

The calculated transition energy in solution, 4.76 and 4.81 eV (nonpolarizable and polarizable solvent, respectively), is overestimated with respect to some experimental data published in the literature, such as for instance 4.35 and 4.40 eV for pCA^{-} in neutral aqueous solution[11] and for its methyl ether derivative in methanol solution,[10] respectively. Results were not improved when the electronic solvent polarization was considered. In fact, during the polarization, there is a mixing of roots that makes the interpretation of results even harder. It seems that further studies are needed in order to clarify the problems found in the description of the carboxylate monoanion.

If one takes as valid the experimental data for carboxylate in gas phase, 2.88 eV, the final experimental solvent shift would be a blue shift of 1.47 eV in contrast with the bathocromic displacement obtained in our study (0.3 eV). In our opinion, so large an experimental blue shift is not realistic considering the characteristics of the studied system and the observed variation of the electronic density during the transitions. Given the agreement between experimental and theoretical values of the transition energies in water solution, this difference is attributed to the discussed discrepancies between experimental and theoretical results for the electronic spectrum in gas phase of this system.

In contrast with the described behavior for the transition to S_2, in the electronic spectrum, the first excited state of the carboxylate anion is shifted toward larger energies when passing from gas phase to water solution; consequently, a blue shift (0.22 eV) is obtained.

3.3. Dianionic Species. Finally, the solvent effect on the structure, charge distribution and electronic spectra of the double anionic form of the *trans-p*-coumaric acid (pCA^{2-}, see Figure 2) was studied. It is important to remark that the pCA^{2-} species is unstable in gas phase and would suffer spontaneous autoionization.[81] However, the interaction with the solvent increases the ionization potential permitting the existence of pCA^{2-} in water solution.

3.3.1. Solvent-Induced Differences in the Structure and Charge Distribution. In order to have a structure with which to compare the changes induced by the solvent, we have performed calculations for pCA^{2-} in gas phase. The ground state presents bond lengths intermediate between those corresponding to the phenolate and carboxylate monoanionic isomers. Whereas the phenolic end looks similar to the phenolate anion (C1−O10, C2−C3 and C5−C6 present double bond character such as the quinolic form of the phenolate anion), the rest of the molecule is more similar to the carboxylate anion (C4−C7 and C8−C9, on the one hand, and C7−C8, on the other hand, are clear single and double bonds respectively).

dx.doi.org/10.1021/ct400145z | J. Chem. Theory Comput. 2013, 9, 4481−4494

In solution, the most significant changes in the geometry are related with the formation of hydrogen bonds with the solvent molecules, and consequently, with the parts of the molecule more exposed to this interaction. In this way C1−O10, C9−O11, and C9−O12 bonds show significant length increase whereas the rest of the system presents the opposite behavior.

Due to the dianionic character of the system, the ground-state dipole moment does not experience significant changes in solution compared to the gas-phase value (Tables 7 and 8), as

Table 8. Dipole Moment, Vertical Transition Energy, Oscillator Strength, and Solvent Shift for the Dianion, pCA^{2-}, in Gas Phase and in Water Solution

	gas phase	water solution	exp
	Dipole Moment (D)		
S_0	4.87	4.78	
S_1	4.72	13.49	
S_2	11.45	4.53	
	Vertical Transition (eV)		
$(S_0 \rightarrow S_1)$	3.45	3.75	3.71[a]
$(S_0 \rightarrow S_2)$	3.96	3.81	
	Oscillator Strength		
$(S_0 \rightarrow S_1)$	0.08	0.66	
$(S_0 \rightarrow S_2)$	0.61	0.07	
	Solvent Shift (kcal/mol)		
$(S_0 \rightarrow S_1)$		−4.77	

[a]Ref 12.

the solvent interacts strongly at both sides of the solute where the charged oxygens are located. As a consequence of the solute−solvent interaction, charges over the terminal oxygens of the solute are increased in agreement with the preference for localized charges in solution. O11 (−0.68 *e*) and O12 (−0.69 *e*) show equivalent negative charges slightly lower than that corresponding to the O10 atom (−0.77 *e*). This fact translates into small differences in the radial distribution functions displayed in Figure 9. The three radial distribution functions are

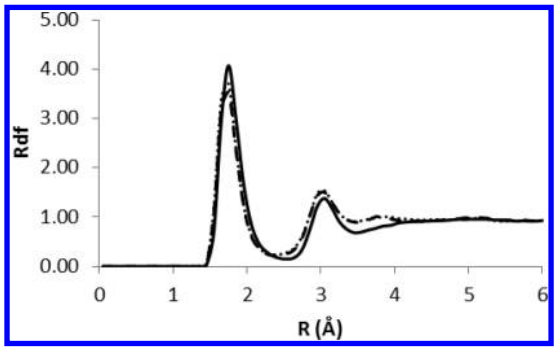

Figure 9. Radial distribution function (rdf) of the *p*-coumaric dianion in water solution. O10-water hydrogen (full line), O11-water hydrogen (dashed line), O12-water hydrogen (dotted line).

well-structured functions with maxima located at the same distances, the O10−Hw function shows a first maximum slightly higher and a first minimum deeper than the other two functions.

3.3.2. Solvent Shifts on the Electronic Spectra of the Dianionic Form. In gas phase, the bright state is the S_2 state that corresponds to a H → L transition, whereas the S_1 state implies the transition H → L + 1. Figure 10 collects the

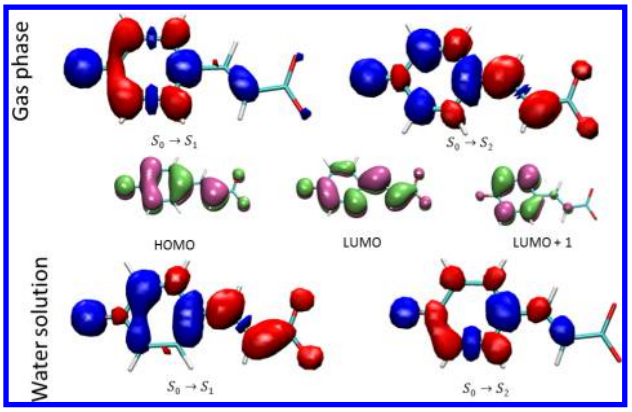

Figure 10. Three-dimensional maps of the studied transitions in gas phase and in water solution of the dianion pCA^{2-}. The electronic flux goes from the blue part to the red one. The involved orbitals are depicted as well in green and mauve colors.

involved orbitals during vertical transitions in gas phase and in solution. Only the states below the bright one have been considered. In general, orbitals are quite similar to those previously analyzed for monoanionic and neutral species. From the analysis of the Mulliken charges (Table 7), it follows that the transition to the bright excited state in gas phase $(S_0 \rightarrow S_2)$ involves the displacement of −0.3 *e* from the phenolic ring mainly to the central part of the molecule (−0.26 *e*) and in a somewhat lower extent to the carboxylic end. The $(S_0 \rightarrow S_1)$ transition hardly changes the electron distribution of the molecule. The order of the excited states and the topology of the involved orbitals are completly coincident with the recently published theoretical data for pCA^{2-} in gas phase.[81] Equally, Boggio-Pasqua et al.[81] found that the promotion of one electron into the LUMO orbital corresponds to a negative charge displacement (−0.28 *e*) from the ring onto the tail of the chromophore. With respect to the transition energies values, our results 3.45 and 3.96 eV for S_1 and S_2, respectively, are slightly larger than those reported by these authors (3.22 and 3.67 eV) who use a lower calculation level (SA(2)-CAS(12,11)-PT2//CASSCF(12,11)/6-31G*). Our calculations were run at SA(10)-CAS(14,12)-PT2//B3LYP/cc-pVDZ level. In any case, the gap between S_1 and S_2 remains practically constant around 0.5 eV at both levels of calculation.

In solution, the charge distribution of the ground state is slightly modified and the negative charge increases at the carboxylic end. Now the bright excited state is stabilized and becomes the first excited state as the charge displacement involved in this transition (−0.35 *e* in solution) is favored by the solvent. The S_2 excited state corresponds now to the H → L + 1 transition. In an attempt to mimic the solvent environment Boggio-Pasqua el al.[81] studied the pCA^{2-} dianion surrounded by eight water molecules. They found a stabilization of the H → L transition, but it was not enough to cause the inversion between S_1 and S_2 states in solution. In our case, the S_1 bright state is more stabilized than the ground state and consequently a red solvent shift of around 0.22 and 0.23 eV (nonpolarizable and polarizable solvent, respectively) is obtained in water solution. This fact evidences the importance that the bulk solvent contribution has in this system. The calculated transition energy in solution (3.75 and 3.73 eV for non-polarizable and polarizable solvent, respectively) is in very good agreement with the experimental data recently published by Putschögl et al.[12] where the *trans-p*-coumaric acid in aqueous

dx.doi.org/10.1021/ct400145z | J. Chem. Theory Comput. 2013, 9, 4481−4494

solution at pH > 10 showed an absorption maximum at around 3.71 eV. It is worth noting the different contribution of the electronic solvent polarization component to the final value of the solvent shift in neutral and ionic forms. In pCA, because of the charge transfer nature of the transitions, there is a very important change in the dipole moment of the molecule and the excited state is stabilized when the solvent polarizes. In ionic forms, the larger contribution to the solvent shift comes from the charge−potential term, the dipole−reaction field term playing only a marginal role. In this latter case, the solvent polarization hardly contributes to the final value of the solvent shift.

3.4. Role of the Deprotonation. By comparing the energetic results obtained for pCA^{2-}, pCA^{-}, and pCA, the role of deprotonation on the absorption spectrum can be analyzed. We will restrict ourself to the changes showed by the bright excited state. In Figure 11, it is shown a global picture of the evolution of the transition energy with the protonation state and the environment. In gas phase, when passing from the neutral form to the phenolate monoanion, there is an important decrease of the transition energy. The red shift is calculated to be 1.6 eV (from 4.49 to 2.89 eV), and the bright state is the first excited state for the deprotonated form. This result is in very good agreement with the CC2 and EOM-CCSD calculations of Gromov et al.[17] on the *p*-coumaric thio-methyl ester (pCTM). In this molecule, the deprotonation entails a shift of about 1.7 eV. It is notable the good agreement between the transition energies calculated for pCTM and pCA (4.59 and 4.56 eV for the neutral forms and 2.89 and 2.90 eV for the phenolate isomers). This fact supports the validity of pCA as a simple model for the PYP chromophore. Besides, the deprotonation and formation of the phenolate isomer in gas phase leads to transitions energies very close to the PYP absorption maximum of 2.78 eV. According to these results, the protein environment seems to provide the chromophore a set of interactions that, as a whole, reproduces the gas-phase conditions. This is supported by experimental observations carried out for both the PYP and GFP (green fluorescent protein) chromophores.[11,82] Nevertheless, this apparent resemblance could have its origin in a combination of blue and red shifts related to the disruption of the chromophore planarity inside the protein and the intermolecular interactions between them.[83] A subsequent deprotonation would lead to the dianionic species with a calculated blue shift of ca. 1 eV.

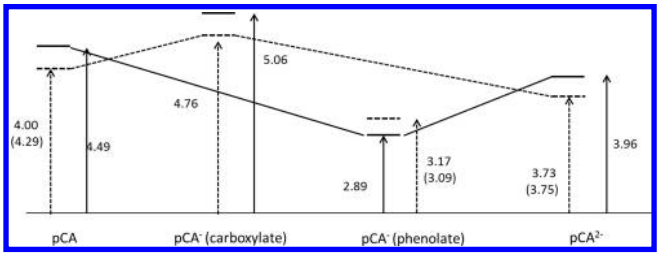

Figure 11. Evolution of the transition energies (in eV) for the *trans-p*-coumaric acid with the protonation state and the environment. Gas phase (full line) and water solution (dashed line). For the in-solution transition energies, the effect of the electronic solvent polarization has been included (values in parentheses correspond to those obtained without this contribution).

In water solution, a red shift of 1.2 eV is obtained during the passsage from the neutral to the phenolate monoanion form. However, in the case of pCA, this comparison is not adequate due to the different stability of the monoanionic forms (phenolate and carboxylate) in gas phase and in water solution. Thus, according with the experimental study of Putschögl et al.,[12] by passing from acidic (pH < 4) to neutral conditions (4 < pH < 9), a blue shift of 0.38 eV is achieved. This shift is due to the deprotonation of the neutral form and the formation of the carboxylate monoanion, the most stable anion in water solution. Our calculations lead to a blue shift of 0.76 eV. The origin of this overestimation can be found in the existing difference between the experimental and calculated in-solution transition energies for the carboxylate monoanion (4.35 vs 4.76, respectively). This species shows special difficulties to be described both in gas phase and in solution. With the purpose of casting some light on this problem, further studies are being performed.

By increasing the basicity, a subsequent deprotonation of the carboxylate monoanion will lead to the dianion pCA^{2-} with the effect of red-shifting the absorption of the chromophore. Regarding the experiments, at least two sets of results are available in the literature. Putschölg et al.[12] published a red shift of 0.67 eV resulting from the difference between 4.38 and 3.71 eV corresponding to the carboxylate anion, existing at pH between 4 and 9 approximately, and the dianion at alkaline conditions, respectively. On the other hand, Nielsen et al.[11] reported a value for the red shift of 0.66 eV, with an absorption maximum for the chromophore of 4.35 and 3.69 eV in neutral and alkaline solutions, respectively. Our results reproduce the experimental trend, but the calculated red shift (1.00 eV) is overestimated. This happens because, as it has been indicated before, transition energies for the dianionic molecule are in better agreement with the experimental data than those obtained for the carboxylate anion. In fact, if we take as a reference value the corresponding to the neutral form in solution (4.00 eV) then the calculated neutral−dianionic red shift is very well reproduced.

4. CONCLUSIONS

We have compared the properties and absorption spectra of the different protonated states of the structurally simplest model of the photoactive yellow protein chromophore, the *trans-p*-coumaric acid (pCA), in gas phase and in water solution. Even though, in the protein, the chromophore is assumed to be in its phenolate monoanionic form, when it is found in solution a pH control can provide neutral, monoanionic, and dianionic species. The pCA molecule has two hydrogens susceptible of deprotonation being the carboxylic one more acidic than the phenolic in water solution. With this, in this medium, the more stable monoanionic form is the carboxylate, whereas in gas phase it is the phenolate. For this reason, it is necessary to be very careful when absorption maxima in different media are compared.

The calculated transition energies at SA(10)-CAS(14,12)-PT2//B3LYP/cc-pVDZ level are in quite good agreement with the available experimental data. The main difference is found when comparing theoretical and experimental absorption maxima for the carboxylate monoanion in gas phase. The experiment places this absorption at 2.88 eV[10] (the same value as for the phenolate monoanion). Our calculated transition energies in gas phase are 5.06 eV for carboxylate and 2.89 eV for phenolate. Since the experimental transition energy for carboxylate in water solution is found at around 4.35 eV,[12] the solvent effect leads to an experimental blue shift of 1.47 eV. In

our opinion, this shift is too large taking into account the characteristics of the system and the electronic density variation during the transitions. In fact, our calculations lead to an opposite solvent effect; that is, we find a red shift of 0.3 eV. Our results support the idea that a revision or reinterpretation of the experimental data for the carboxylate monoanion in gas phase is required in order to clarify this problem.

For all the studied species, the bright state is a $\pi \rightarrow \pi^*$ transition involving a charge displacement along the system. For the neutral form, the transition involves an increase of the dipole moment of the excited state, a fact that leads to a larger stabilization of the excited state in water solution and consequently a bathochromic shift of the absorption maximun in solution. Phenolate and carboxylate monoanions show different behavior with respect to solvation. On the one hand, the phenolate monoanion in gas phase shows a displacement of the charge from the phenolic oxygen to the rest of the system during the transition, and this is enhanced in water solution. As the displacement involves a decrease of the dipole moment, the ground state is better stabilized than the excited one, and a final solvent blue shift is achieved. On the other hand, the carboxylate monoanion shows in gas phase an opposite displacement for the negative charge that moves from the COO^- toward the phenolic ring. The solvent hinders this displacement, as it solvates more effectively localized charges; in solution, therefore, the sense of the charge displacement is inverted, and the dipole moment of the excited state becomes higher than the ground state one. In this case, a solvent red shift is found. Finally, for the dianionic species the electronic transition to the bright state involves a charge displacement from the phenolic part toward the rest of the system with an associated increase of the dipole moment. This displacement is enhanced in water solution, the excited state is more effectively solvated than the ground state, and a final solvent red shift is shown.

With respect to the effect of the electronic solvent polarization in the transition energies and solvent shift values two cases can be distinguished. In neutral species, the polarization contribution depends on the state nature. That is, it is relevant in those cases in which there exists a significant charge displacement between the ground and the excited state. On the contrary, in ionic forms (mono- and dianionic species), the larger contribution comes from the charge−potential term and, in general, solvent polarization has only a minor influence.

■ ASSOCIATED CONTENT

Supporting Information

Supporting Information available with the following data. Gas phase and in solution geometries for the ground state of all studied species. Mulliken charges and dipole moments for the ground and excited states of all the forms in gas phase and in solution. Transition energies, oscillator strength, and solvent shift for the different monoanions in gas phase and water solution. Performance of different basis sets in gas phase and in solution. This information is available free of charge via the Internet at http://pubs.acs.org.

■ AUTHOR INFORMATION

Corresponding Authors

*E-mail: maguilar@unex.es.
*E-mail: memartin@unex.es.

Notes

The authors declare no competing financial interest.

■ ACKNOWLEDGMENTS

This work has been supported by the CTQ2011-25692 Project from the Ministerio de Economía y Competitividad of Spain, cofinanced by the European Regional Development Fund (ERDF), and by the Consejería de Economía, Comercio e Innovación of the Gobierno de Extremadura. I.F.G. acknowledges the Gobierno de Extremadura and the European Social Fund for financial support. A.M.L. acknowledges financial support from the Juan de la Cierva subprogramme of the Ministerio de Ciencia e Innovación of Spain. The authors also thank the Fundación Computación y Tecnologías Avanzadas de Extremadura (COMPUTAEX) for additional computation resources.

■ REFERENCES

(1) Meyer, T. E. *Biochim. Biophys. Acta* **1985**, *806*, 175.
(2) Larsen, D. S.; van Grondelle, R. *ChemPhysChem* **2005**, *6*, 828.
(3) Sprenger, W. W.; Hoff, W. D.; Armitage, J. P.; Hellingwerf, K. J. *J. Bacteriol.* **1993**, *175*, 3096.
(4) Kim, M.; Mathies, R. A.; Hoff, W. D.; Hellingwerf, K. J. *Biochemistry* **1995**, *34*, 12669.
(5) Kort, R.; Vonk, H.; Xu, X.; Hoff, W. D.; Crielaard, W.; Hellingwerf, K. J. *FEBS Lett.* **1996**, *382*, 73.
(6) Xie, A.; Hoff, W. D.; Kroon, A. R.; Hellingwerf, K. J. *Biochemistry* **1996**, *35*, 14671.
(7) Unno, M.; Kumauchi, M.; Sasaki, J.; Tokunaga, F.; Yamaguchi, S. *J. Am. Chem. Soc.* **2000**, *122*, 4233.
(8) Genik, U. K.; Soltis, S. M.; Kuhn, P.; Canestrelli, I. L.; Getzoff, E. D. *Nature* **1998**, *392*, 206.
(9) Kukura, P.; McCamant, D. W.; Yoon, S.; Wandschneider, D. B.; Mathies, R. A. *Science* **2005**, *310*, 1006.
(10) Rocha-Rinza, T.; Christiansen, O.; Rajput, J.; Gopalan, A.; Rahbek, D. B.; Andersen, L. H.; Bochenkova, A. V.; Granovsky, A. A.; Bravaya, K. B.; Nemukhim, A. V.; Chistiansen, K. L.; Nielsen, M. B. *J. Phys. Chem. A* **2009**, *113*, 9442.
(11) Nielsen, I. B.; Boyé-Péronne, S.; El Ghazaly, M. O. A.; Kristensen, M. B.; Nielsen, S. B.; Andersen, L. H. *Biophys. J.* **2005**, *89*, 2597.
(12) Putschögl, M.; Zirak, P.; Penzkofer, A. *Chem. Phys.* **2008**, *343*, 107.
(13) Lammich, L.; Rajput, J.; Andersen, L. H. *Phys. Rev. E* **2008**, *78*, 051916.
(14) Ma, Y.; Rohlfing, M.; Molteni, C. *J. Chem. Theory Comput.* **2010**, *6*, 257.
(15) Zuev, D.; Bravaya, K. B.; Crawford, T. D.; Lindh, R.; Krilov, A. I. *J. Chem. Phys.* **2011**, *134*, 034310.
(16) Gromov, E.; Burghardt, I.; Hynes, I.; Köppel, H.; Cederbaum, L. S. *J. Photochem. Photobiol., A* **2007**, *190*, 241.
(17) Gromov, E.; Burghardt, I.; Köppel, H.; Cederbaum, L. S. *J. Am. Chem. Soc.* **2007**, *129*, 6798.
(18) Riss, U. V.; Meyer, H.-D. *J. Phys. B* **1993**, *26*, 4503.
(19) Jolicard, G.; Austin, E. *J. Chem. Phys. Lett.* **1985**, *121*, 106.
(20) Aguilar, J.; Combes, J. M. *Commun. Math. Phys.* **1971**, *22*, 269.
(21) Balsev, E.; Combes, J. M. *Commun. Math. Phys.* **1971**, *22*, 280.
(22) Simon, B. *Commun. Math. Phys.* **1972**, *27*, 1.
(23) Reinhardt, W. P. *Annu. Rev. Phys. Chem.* **1983**, *33*, 223.
(24) Zuev, D.; Bravaya, K. B.; Makarova, M. V.; Krilov, A. I. *J. Chem. Phys.* **2011**, *135*, 194304.
(25) Yoda, M.; Houjou, H.; Inoue, Y.; Sakurai, M. *J. Phys. Chem. B* **2001**, *105*, 9887.
(26) Yoda, M.; Inoue, Y.; Sakurai, M. *J. Phys. Chem. B* **2003**, *107*, 14569.
(27) Chiba, M.; Fedorov, D. G.; Kitaura, K. *J. Comput. Chem.* **2008**, *29*, 2667.

(28) Wang, Y.; Li, H. *J. Chem. Phys.* **2010**, *133*, 034108.
(29) Fdez. Galván, I.; Sánchez, M. L.; Martín, M. E.; Olivares del Valle, F. J.; Aguilar, M. A. *Comput. Phys. Commun.* **2003**, *155*, 244.
(30) Sánchez, M. L.; Aguilar, M. A.; Olivares del Valle, F. J. *J. Comput. Chem.* **1997**, *18*, 313.
(31) Sánchez, M. L.; Martín, M. E.; Aguilar, M. A.; Olivares del Valle, F. J. *J. Comput. Chem.* **2000**, *21*, 705.
(32) Sánchez, M. L.; Martín, M. E.; Fdez. Galván, I.; Olivares del Valle, F. J.; Aguilar, M. A. *J. Phys. Chem. B* **2002**, *106*, 4813.
(33) Angyán, J. G. *J. Math. Chem.* **1992**, *10*, 93.
(34) Tapia, O. In Theoretical Treatment of Large Molecules and Their Interactions; Maksic, Z. B., Ed.; Springer-Verlag: Berlin, 1991; Vol. *4*; p 435.
(35) Warshel, A.; Levitt, M. *J. Mol. Biol.* **1976**, *102*, 227.
(36) Martín, M. E.; Sánchez, M. L.; Corchado, J. C.; Muñoz-Losa, A.; Fdez. Galván, I.; Olivares del Valle, F. J.; Aguilar, M. A. *Theor. Chem. Acc.* **2011**, *128*, 783.
(37) Coutinho, K.; Rivelino, R.; Georg, H. C.; Canuto, S. In *Solvation Effects on Molecules and Biomolecules. Computational Methods and Applications*; Canuto, S., Ed.; Springer: New York, 2008.
(38) Allen, M. P.; Tildesley, D. J. *Computer Simulation of Liquids*; Oxford University Press: London, 1987.
(39) Ten-no, S.; Hirata, F.; Kato, S. *Chem. Phys. Lett.* **1993**, *214*, 391.
(40) Sato, H.; Hirata, F.; Kato, S. *J. Chem. Phys.* **1996**, *105*, 1546.
(41) Understanding Chemical Reactivity. In *Molecular Theory of Solvation*; Hirata, F., Ed.; Kluwer Academic Publisher: Dordrecht, 2004.
(42) Coutinho, K.; Georg, H. C.; Fonseca, T. L.; Ludwig, V.; Canuto, S. *Chem. Phys. Lett.* **2007**, *437*, 148.
(43) Nakano, H.; Yamamoto, T. *J. Chem. Phys.* **2012**, *136*, 134107.
(44) Zhou, X.; Kaminski, J. W.; Wesolowski, T. A. *Phys. Chem. Chem. Phys.* **2011**, *13*, 10565.
(45) Okuyama-Yoshida, N.; Nagaoka, M.; Yamabe, T. *Int. J. Quantum Chem.* **1998**, *70*, 95.
(46) Okuyama-Yoshida, N.; Kataoka, M.; Nagaoka, M.; Yamabe, T. *J. Chem. Phys.* **2000**, *113*, 3519.
(47) Hirao, H.; Nagae, Y.; Nagaoka, M. *Chem. Phys. Lett.* **2001**, *348*, 350.
(48) Zhang, Y.; Liu, H.; Yang, W. *J. Chem. Phys.* **2000**, *112*, 3483.
(49) Fdez. Galván, I.; Sánchez, M. L.; Martín, M. E.; Olivares del Valle, F. J.; Aguilar, M. A. *J. Chem. Phys.* **2003**, *118*, 255.
(50) Zwanzig, W. R. *J. Chem. Phys.* **1954**, *22*, 1420.
(51) Gao, J. *J. Comput. Chem.* **1997**, *18*, 1061.
(52) Thompson, M. A. *J. Phys. Chem.* **1996**, *100*, 14492.
(53) Martín, M. E.; Muñoz-Losa, A.; Fdez. Galván, I.; Aguilar, M. A. *J. Chem. Phys.* **2004**, *121*, 3710.
(54) Martín, M. E.; Sánchez, M. L.; Olivares del Valle, F. J.; Aguilar, M. A. *J. Chem. Phys.* **2000**, *113*, 6308.
(55) Muñoz-Losa, A.; Fdez. Galván, I.; Martín, M. E.; Aguilar, M. A. *J. Phys. Chem. B* **2006**, *110*, 18064.
(56) Becke, A. D. *J. Chem. Phys.* **1993**, *98*, 5648.
(57) Kohn, W.; Sham, L. *J. Phys. Rev.* **1965**, *140*, A1133.
(58) Frisch, M. J.; Trucks, G. W.; Schlegel, H. B.; Scuseria, G. E.; Robb, M. A.; Cheeseman, J. R.; Scalmani, G.; Barone, V.; Mennucci, B.; Petersson, G. A.; Nakatsuji, H.; Caricato, M.; Li, X.; Hratchian, H. P.; Izmaylov, A. F.; Bloino, J.; Zheng, G.; Sonnenberg, J. L.; Hada, M.; Ehara, M.; Toyota, K.; Fukuda, R.; Hasegawa, J.; Ishida, M.; Nakajima, T.; Honda, Y.; Kitao, O.; Nakai, H.; Vreven, T.; Montgomery, J. A., Jr.; Peralta, J. E.; Ogliaro, F.; Bearpark, M.; Heyd, J. J.; Brothers, E.; Kudin, K. N.; Staroverov, V. N.; Kobayashi, R.; Normand, J.; Raghavachari, K.; Rendell, A.; Burant, J. C.; Iyengar, S. S.; Tomasi, J.; Cossi, M.; Rega, N.; Millam, J. M.; Klene, M.; Knox, J. E.; Cross, J. B.; Bakken, V.; Adamo, C.; Jaramillo, J.; Gomperts, R.; Stratmann, R. E.; Yazyev, O.; Austin, A. J.; Cammi, R.; Pomelli, C.; Ochterski, J. W.; Martin, R. L.; Morokuma, K.; Zakrzewski, V. G.; Voth, G. A.; Salvador, P.; Dannenberg, J. J.; Dapprich, S.; Daniels, A. D.; Farkas, .; Foresman, J. B.; Ortiz, J. V.; Cioslowski, J.; Fox, D. J. *Gaussian 09*, Revision B.0.; Gaussian Inc.: Wallingford, CT, 2009.
(59) Refson, K. *Comput. Phys. Commun.* **2000**, *126*, 310.
(60) Aquilante, F.; de Vico, L.; Ferré, N.; Ghigo, G.; Malmquist, P. Å.; Neogrády, P.; Pedersen, T.; Pitonak, M.; Reiher, M.; Roos, B. O.; Serrano-Andrés, L.; Urban, M.; Veryazov, V.; Lindh, R. *J. Com.* **2010**, *31*, 224.
(61) Roos, B. O. *In Ab Initio Methods in Quantum Chemistry*; Lawley, K. P., Ed.; Wiley: New York, 1987.
(62) Roos, B. O.; Fülscher, M. P.; Malmqvist, P. Å.; Merchán, M.; Serrano-Andrés, L. In *Quantum Mechanical Electronic Structure Calculations with Chemical Accuracy*; Langhorff, S. R., Ed.; Kluwer: Dordrecht, 1994.
(63) Andersson, K.; Malmquist, P. Å.; Roos, B. O. *J. Chem. Phys.* **1992**, *96*, 1218.
(64) Malmquist, P. Å.; Roos, B. O. *Chem. Phys. Lett.* **1989**, *155*, 189.
(65) Fdez. Galván, I.; Martín, M. E.; Muñoz-Losa, A.; Aguilar, M. A. *J. Chem. Theory Comput.* **2009**, *5*, 341−349.
(66) Fdez. Galván, I.; Martín, M. E.; Aguilar, M. A. *J. Chem. Theory Comput.* **2010**, *6*, 2445−2454.
(67) Fdez. Galván, I.; Martín, M. E.; Muñoz-Losa, A.; Sánchez, M. L.; Aguilar, M. A. *J. Chem. Theory Comput.* **2011**, *7*, 1850−1857.
(68) Fdez. Galván, I.; Martín, M. E.; Muñoz-Losa, A.; Aguilar, M. A. *J. Chem. Theory Comput.* **2011**, *7*, 3694−3701.
(69) Jorgensen, W.; Maxwell, D. S.; Tirado-Rives, J. *J. Am. Chem. Soc.* **1996**, *118*, 11225.
(70) Chirlian, L. E.; Francl, M. M. *J. Comput. Chem.* **1987**, *8*, 894.
(71) Breneman, M.; Wiberg, K. B. *J. Comput. Chem.* **1990**, *11*, 316.
(72) Jorgensen, W. L.; Chandrasekhar, J.; Madura, J. D.; Impey, R. W.; Klein, M. L. *J. Chem. Phys.* **1983**, *79*, 926.
(73) Hoover, W. G. *Phys. Rev. A* **1985**, *31*, 1695.
(74) Schaftenaar, G.; Noordik, J. H. *J. Comput.-Aided Mol. Des.* **2000**, *14*, 123.
(75) Gromov, E. V.; Burghardt, I.; Köppel, H.; Cederbaum, L. S. *J. Phys. Chem. A* **2005**, *109*, 4623.
(76) Chaehyuk, K.; Levine, B.; Toniolo, A.; Manohar, L.; Olsen, S.; Werner, H.-J.; Martínez, T. J. *J. Am. Chem. Soc.* **2003**, *125*, 12710.
(77) Sergi, A.; Grüning, M.; Ferrario, M.; Buda, F. *J. Phys. Chem. B* **2001**, *105*, 4386.
(78) Beerepoot, M. T. P.; Steindal, A. H.; Kongsted, J.; Brandsdal, B. O.; Frediani, L.; Ruud, K.; Olsen, J. M. H. *Phys. Chem. Chem. Phys.* **2013**, *15*, 4735.
(79) Slipchenko, L. V. *J. Phys. Chem. A* **2010**, *114*, 8824.
(80) Sneskov, K.; Schwabe, T.; Christiansen, O.; Kongsted, J. *Phys. Chem. Chem. Phys.* **2011**, *13*, 18551.
(81) Boggio-Pasqua, M.; Groenhof, G. *J. Phys. Chem. B* **2012**, *115*, 7021.
(82) Lammich, L.; Petersen, M. A.; Nielsen, M. B.; Andersen, L. H. *Biophys. J.* **2007**, *92*, 201.
(83) Rocha-Rinza, T.; Sneskov, K.; Christiansen, O.; Ryde, U.; Kongsted, J. *Phys. Chem. Chem. Phys.* **2011**, *13*, 1585.